THE ASTROPHYSICAL JOURNAL 243:175–183, 1981 January 1

A MODEL REFLECTION NEBULA IN THE FAR-INFRARED

G. A. SHAH
Indian Institute of Astrophysics, Bangalore
AND
K. S. KRISHNA SWAMY
Tata Institute of Fundamental Research, Bombay
Received 1980 March 3; accepted 1980 July 8

ABSTRACT

We have considered a model of a reflection nebula with the star within a homogeneous plane-parallel slab of 1 pc thickness. The model is intended to imitate the Merope reflection nebula. The illuminating star is located at 0.35 pc from the front surface of the nebula. The size distribution of the grains has been incorporated. Using the radiation balance equation for input and output powers, we have calculated the grain temperature as a function of size, offset angle, and position of each grain within the nebula. These results have been used to calculate the expected infrared fluxes in the wavelength range 1–100 μm with the offset angle as parameter. The results for ice, graphite, and silicate grains show some interestingly distinguishable structures in the flux versus wavelength curves. A rough estimate for the highest flux turns out to be $F \sim (5 \times 10^{-12\pm1})\, n_{\rm H}$ W m^{-2} μm^{-1} sr^{-1} corresponding to offset angle $\phi = 0°$, $n_{\rm H}$ being the hydrogen number density. The proportionality to $n_{\rm H}$ occurs because we have assumed a constant ratio of the grain number density to $n_{\rm H}$. It is not unreasonable to expect observable infrared fluxes in the appropriate wavelength range in the direction toward the Merope reflection nebula. In particular, from the observational point of view, we predict that the best results on the strongest infrared radiation from the Merope reflection nebula can occur near about 40 μm.

Subject headings: infrared: sources — interstellar: matter — nebulae: reflection

I. INTRODUCTION

Among the galactic infrared objects observed so far, reflection nebulae are a rarity. In a recent overview on infrared space astronomy, Low (1977) stated that many new infrared sources are likely to be discovered in the near future as further improvements in instruments are made. Even in cool interstellar regions where there is no local ultraviolet radiation source, one would expect the ambient ultraviolet radiation field to be largely degraded into far-infrared thermal emission by interstellar grains within the clouds. Greenberg (1978) and Kolesnik (1978) demonstrated that the far-infrared flux at $\sim$300 μm from dense dust clouds can be detected with modern capabilities of infrared survey instruments, including those aboard a satellite planned in the near future. In H II regions associated with dark clouds, one expects the far-infrared continuum to be peaked in the 50–150 μm range because the dust grains in and around H II regions achieve somewhat higher temperatures by absorbing nearly all the energy from the associated O–B stars. One may imagine a reflection nebula to be a case intermediate between these two types of objects. A reflection nebula is therefore a more suitable object for studying the properties of interstellar grains.

Emerson, Furniss, and Jennings (1975) observed such a source of far-infrared radiation in 40–350 μm band in the direction of the reflection nebula and molecular cloud NGC 2023. In this source, as in KL and OMC-2, the dust is mixed with gas in a predominantly neutral state. Thus the interpretation is much simpler compared to the case of H II infrared regions.

The reflection nebulosity associated with Merope (23 Tau) in the Pleiades cluster has received considerable attention in recent years in *UBV* photometry (Elvius and Hall 1966, 1967; Greenberg and Roark 1967; Shah 1974, 1977*a*, *b*; Markkanen 1977; Jura 1979; Arny 1977; Voshchinnikov 1977, 1978) and in far-ultraviolet surface brightness studies (Andriesse, Piersma, and Witt 1977; Shah and Krishna Swamy 1978, 1979). However, as mentioned by Savage and Mathis (1979), the subject of the analysis of scattered light and the inferences regarding the star-nebula geometry as well as the candidate grain species are controversial at present.

Jura (1977) has estimated that a sister reflection nebula associated with 20 Tau (Maia) in Pleiades could be a far-infrared source. The measurement of the amount of the far-infrared light may be useful for an independent estimation of average albedo of the grains in the visual and ultraviolet. One may as well be able to discriminate among the various candidate materials for the grains. Therefore, it is of interest to observe the Merope reflection nebula in the far-infrared along with the *UBV* and far-ultraviolet studies.

Here, we propose to study an experimental model of

the Merope reflection nebula in the far-infrared and calculate possible infrared spectra of the thermal radiation emitted by the nebular grains composed of ice, graphite, and olivine silicate materials.

II. MODEL OF THERMAL EMISSION FROM THE REFLECTION NEBULA

We consider a model reflection nebula in the form of a plane-parallel homogeneous slab perpendicular to the line of sight to the illuminating star. In the first attempt here the geometrical case of the star within the nebula (SWN) has been adopted. A detailed model for SWN has been described by Shah and Krishna Swamy (1978) in connection with the theoretical studies of far-ultraviolet surface brightness, colors, and polarization of the Merope reflection nebula. Since we intend to study possible far-infrared radiation from this nebula, the stellar energy distribution for the attendant star Merope (23 Tau, B6 IV) as given by Andriesse *et al.* has been considered as the original driving source of energy in the far-ultraviolet to near-infrared wavelength range. The grains are assumed to be smooth, homogeneous and isotropic spheres distributed uniformly throughout the nebula. The grain size distribution function has the following normalized form:

$$n(a)da = \frac{cn_0}{a_0} \exp\left[-5(a/a_0)^3\right]da\,, \qquad (1)$$

where a = the radius of the grain, $n(a)da$ = the number of grains in the size range a and $a + da$, n_0 = the total number of grains per cm^3, a_0 = the characteristic size parameter, and $c = 1.914$. The correction for the extinction of stellar flux reaching a grain within the nebula has been taken into account by calculating the appropriate theoretical optical depth.

The nebular slab is divided into a number (N) of elementary slabs. The observer viewing the nebula at an offset angle ϕ with respect to the observer-star direction will receive thermal radiation from all the nebular elements confined within the cone of view defined by the telescope. The temperature of each volume element will depend, among other things, on the distance from the star and the optical depth along the path from the star to the particular volume element. Figure 1 shows schematically the geometrical configuration. The observer's viewing cone intersects a typical elementary slab $LNN'L'$ into a volume element defined by $MNN'M'$ which is a truncated frustum of a cone with elliptical cross sections at the top and bottom. The exact expression for the volume element such as $MNN'M'$ and related equations have been given by Shah and Krishna Swamy (1978). Here we summarize the essential relations in the Appendix. The symbols, notation, and values of some of the quantities are as follows:

D = the distance from the observer to the illuminating star, 126 pc.
H = the perpendicular distance from the star to the front surface of the nebula, 0.35 pc.
T = the thickness of the nebula, 1 pc.
ϕ = the offset angle.
β = the semi-vertex angle of the telescope, 0.0015 radian.
h = the distance of the bottom of a typical elementary slab from the observer.
$\Delta\Omega$ = the solid angle of the telescope, $\pi \tan^2 \beta$.
$m(\lambda) = m'(\lambda) - im''(\lambda)$, complex index of refraction of the grain material.
λ = the wavelength of light.
$l_1 = OC''$, the distance from the observer to the scattering center within the elementary volume element.
$l_2 = SC''$, the distance from the star to the scattering center.
R_* = the radius of the illuminating star Merope, $= 4\ R_\odot$ with $R_\odot = 6.96 \times 10^{10}$ cm.
$d = SL''$.

The specific values of the quantities mentioned above are held constant throughout the present work. All the grains within an elementary volume $MNN'M'$ are assumed to be located at the scattering center C'' determined according to certain symmetry considerations. The equilibrium temperature attained by a dust grain at C'' is governed by the following equation of radiative balance between input stellar energy and the energy emitted by the grain both per unit time, considering only single scattering:

$$\left(\frac{R_*}{l_2}\right)^2 \int_0^\infty F(T_*, \lambda) e^{-\tau_1} \pi a^2 Q_{\rm abs}\, d\lambda = \int_0^\infty \pi B(T_g, \lambda) 4\pi a^2 Q_{\rm em}\, d\lambda\,, \qquad (2)$$

where

$F(T_*, \lambda)$ = the stellar flux on the surface of the star,
T_* = the surface temperature of the star,
$Q_{\rm abs} = Q_{\rm abs}[a, m(\lambda), \lambda]$ = the absorption efficiency of the grain,
$\pi B(T_g, \lambda)$ = the Planck function for the grain,
T_g = the equilibrium temperature of the grain,
$Q_{\rm em} = Q_{\rm em}(a, m(\lambda), \lambda)$ = the emissivity of the grain,
$\tau_1 = \tau_1[a, m(\lambda), \lambda]$ = the optical depth along SC''.

Equation (2) is a particular case of the more general expression considered by Krishna Swamy (1970) for the case of thermal emission by dust in H II regions. The exact radiation scattering parameters like absorption and extinction efficiencies have been calculated on the basis of the Mie theory (see, for example, van de Hulst 1957). The numerical methods for the Mie theory and the corresponding computer program for arbitrary values of the grain size, wavelength, and complex index of refraction have been adopted from Shah (1977*c*).

In order to facilitate the evaluation of the grain temperature, we first calculate the integral for power radiated by

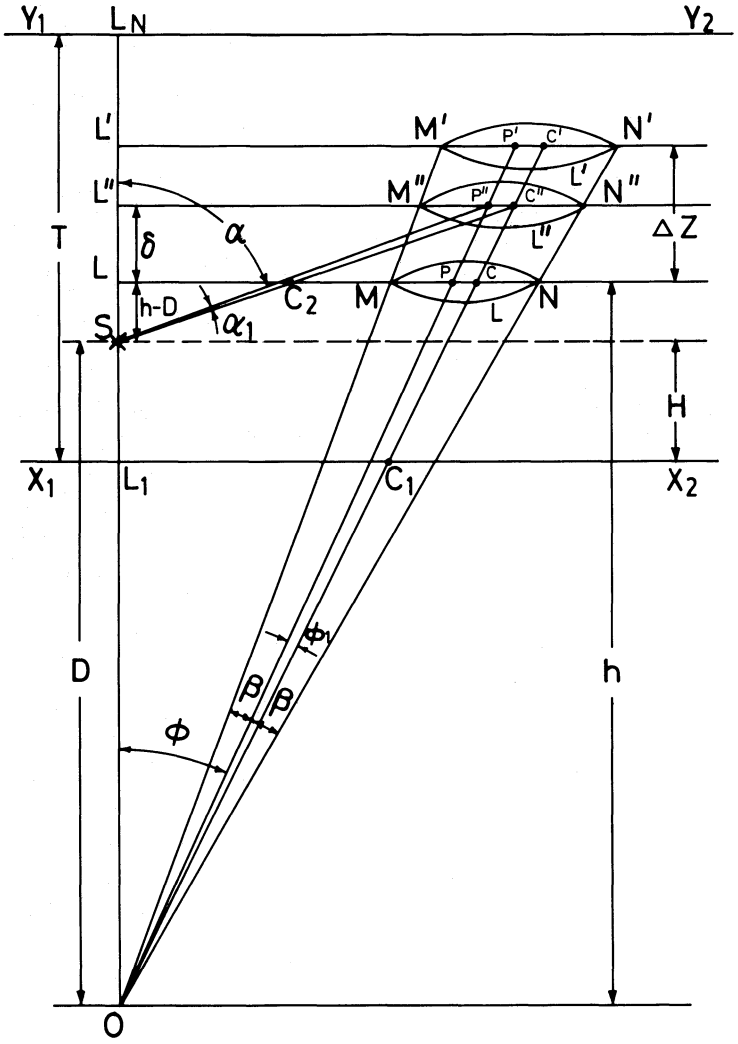

FIG. 1.—Schematic of the model reflection nebula in the form of homogeneous plane-parallel slab.

a grain with radius a_i and temperature $(T_g)_K$ from the following integral:

$$P_{out}[a_i, (T_g)_K] = \int_0^\infty \pi B[(T_g)_K, \lambda] 4\pi a_i^2 Q_{abs}[a_i, m(\lambda), \lambda] d\lambda . \quad (3)$$

The maximum grain radius, a_{max}, is chosen such that $n(a)da$ for a_{max} is negligibly small at the tail of the size distribution curve. The size interval 0 to a_{max} is split up into 23 points with uniform spacing. The temperature values for $(T_g)_K$ are selected in the range 0(25)1000 K. The quantities $Q_{abs}[a_i, m(\lambda), \lambda]$ and $Q_{ext}[a_i, m(\lambda), \lambda]$ have been evaluated while integrating equation (3). Thus, for a given composition of the grain, we prepare in advance a table of $P_{out}[a_i, (T_g)_K]$ for $i = 1$ to 23 and $K = 1$ to 41. This table has been employed for interpolation to compute the actual grain temperature, depending upon the input power to the grain within any volume element in the nebula.

The nebular slab is divided uniformly into N elementary slabs. Thus, viewing at an offset angle ϕ, one encounters N volume elements. The problem is to find the grain temperature for each grain of radius a_i, $i = 1(1)23$, in all the volume elements $\Delta V(\phi, j)$, $j = 1, 2, \ldots, N$, for a fixed value of ϕ. Consider a grain with radius a_i situated within the volume element $\Delta V(\phi, j)$. The input power to such a grain from stellar radiation is given by

$$P_{in}[a_i, \Delta V(\phi, j)] = \int_0^\infty \left(\frac{R_*}{l_2}\right)^2 F(T_*, \lambda) e^{-\tau_1} \pi a_i^2 Q_{abs}[a_i, m(\lambda), \lambda] d\lambda , \quad (4)$$

where symbols have the same meaning as in equation (2). The power P_{in} calculated from equation (4) has been used to interpolate in the table of P_{out} $[a_i, (T_g)_K]$ prepared earlier. We need actually double interpolation since P_{out} is a function of two variables a and T_g. However, single interpolation with respect to T_g only would suffice provided the same set of a_i is used in equations (3) and (4).

The resulting temperature of the grain for particular size a_i and volume element $\Delta V(\phi, j)$ has been denoted by $T_g[a_i, \Delta V(\phi, j)]$ or by T_g for the sake of brevity. By repeated application of this procedure for $i = 1(1)23$ and $j = 1(1)N$, one can thus evaluate the grain temperatures for all radii of the grains in each volume element within the nebula.

Next we can calculate the expected infrared flux from the reflection nebula. The grain number density within the nebula has been assumed to be

$$n_0 = 10^{-12} n_{\rm H} \ {\rm cm}^{-3} , \quad (5)$$

where $n_{\rm H}$ = the hydrogen number density in the nebula. Although we have set $n_{\rm H} = 1$, the densities in the range of $3 \lesssim n_{\rm H} \lesssim 10^3$ are quite possible (Watson 1975).

The infrared flux, integrated over the grain size and summed over all volume elements along the line of sight at an offset angle ϕ, received in the telescope aperture can now be expressed by

$$F_{\rm IR}(\phi, a_0, \lambda) = \sum_{j=1}^{N} \frac{\Delta V(\phi, j)}{4\pi {l_{1j}}^2} \times \int_0^\infty n(a)\pi B(T_g, a, \lambda) Q_{\rm abs} 4\pi a^2 e^{-\tau_2} da , \quad (6)$$

where τ_2 is the optical depth along the portion l_{1R} of the ray trajectory lying within the reflection nebula, l_{1j} = the distance between the volume element $\Delta V(\phi, j)$ and the observer. Note that $l_{1R} \ll l_{1j}$. The characteristic grain size parameter a_0 in the size distribution function has the following values throughout: $a_0 = 0.5$ μm for ice and silicate grains, and $a_0 = 0.2$ μm for graphite grains.

III. SIZE DEPENDENCE OF GRAIN TEMPERATURE WITHIN THE NEBULA

The wavelength-dependent complex indices of refraction $m(\lambda) = m'(\lambda) - im''(\lambda)$ have been used throughout for ice (Field, Partridge, and Sobel 1967; Irvine and Pollack 1968), graphite (Taft and Philipp 1965), and olivine silicate (Huffman and Stapp 1972; Huffman 1975). The calculation of grain temperatures and infrared fluxes has been performed by dividing the nebular slab uniformly into N elementary slabs. N is varied in the range $N = 11(10)41$. This allows one to vary the distance of the star as well as the effects of the temperature gradients within the nebula. Figure 2 shows the equilibrium grain temperatures (T_g) as a function of the grain radius (a) for various selected distances (d) from the illuminating star as parameter. Note that $T_g[a_i, \Delta V(\phi, j)]$ is denoted here simply by T_g. At the end of each curve the number outside the bracket gives $d = SL''$ in pc. The three numbers within the bracket are (i) N, the total number of elementary slabs, (ii) j, the number of the elementary slab in which the grain lies, and (iii) ϕ, the offset angle in minutes of arc. As in the general interstellar medium, for all compositions, the smaller the radius of the grain, the higher the grain temperature, other things like d and ϕ, etc., being equal. The graphite grains attain the highest temperature compared to ice and silicate for the same set of other variables. For instance, considering the curve for

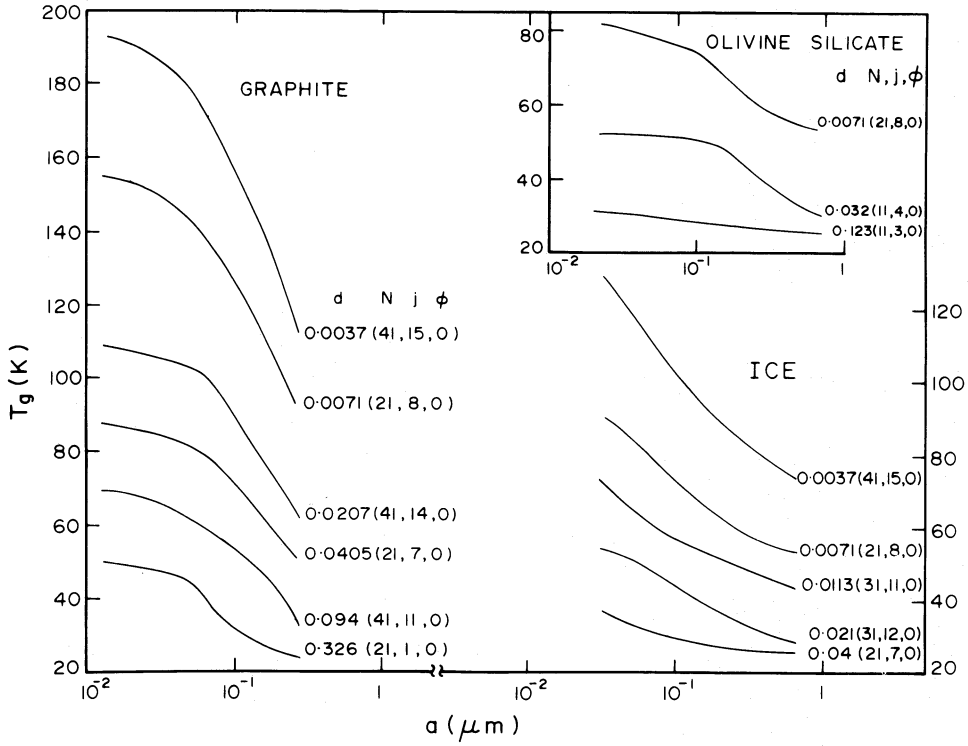

FIG. 2.—Size dependence of the temperature of the grains at various distances (d) from the illuminating star within the nebula. The number outside the bracket gives d; the ones within the bracket are as described in the text.

$d = 0.0071$ pc ($N = 21, j = 8, \phi = 0°$) in Figure 2, as the grain radius a varies from 0.03 μm to 0.3 μm, the grain temperature spans the range of 150 K to 88 K for graphite, 91 K to 59 K for ice, and 81 K to 58 K for silicate. Thus the results in Figure 2 conform to the general trend that the submicron metallic particles are always hotter than the dielectric particles of the same size in the same radiation field. The graphite and ice grains show monotonic variation of T_g; so do olivine silicate grains except that they are somewhat flat in the range of size $a = 0.01$ μm to 0.1 μm for $d = 0.032$ pc and 0.123 pc. In fact, the silicate grain temperature is a very slowly varying function of a for $d = 0.123$. Since the grain temperatures in the present work are much below the evaporation temperature for the three types of grains chosen here, they are expected to survive and emit the infrared radiation beyond 1 μm wavelength.

IV. EXPECTED INFRARED FLUXES FROM THE REFLECTION NEBULA

The expected infrared fluxes, F_{IR}, as a function of wavelength in the range 1–100 μm have been calculated according to equation (6) for offset angles $\phi = 0°(8')16'$. The parameter a_0 in the size distribution function defined by equation (1) has been maintained constant for each candidate material of the grains. The extinction factor $e^{-\tau_2}$ in equation (6), though likely to be small, has been calculated theoretically. Although the minimum distance, d_{min}, of the elementary slab closest to the star varies in general inversely with N, it turns out that $d_{min}(N = 21) < d_{min}(N = 31)$. The main contribution to the infrared flux comes from the volume element closest to the illuminating star.

The results for infrared fluxes due to ice grains with $a_0 = 0.5$ μm have been set out in Figure 3. For $\phi = 0°$, $N = 11$, and $\phi = 8'$, $N = 11(10)41$, two peaks are prominent, one between 40 to 50 μm, and another between 60 and 80 μm. For $\phi = 0°$, $N = 21(10)41$, the second peak becomes inconspicuous. However, at the same time, for $\phi = 0$ and $N = 41$, a new peak shows up at $\lambda \sim 15$ μm. As expected for all compositions of the grains, the infrared flux increases with the decrease in d_{min}. The wavelength of the first peak for $\phi = 0°$ and $8'$ remains almost unchanged at ~ 44 μm and ~ 48 μm, respectively. The maximum infrared flux from the nebula is expected to be $\sim 1.3 \times 10^{-11} n_H$ W m^{-2} μm^{-1} sr^{-1} for $\phi = 0°, N = 41$; and $\sim 1.3 \times 10^{-15} n_H$ W m^{-2} μm^{-1} sr^{-1} for $\phi = 8', N = 11(10)41$. The proportionality to n_H essentially

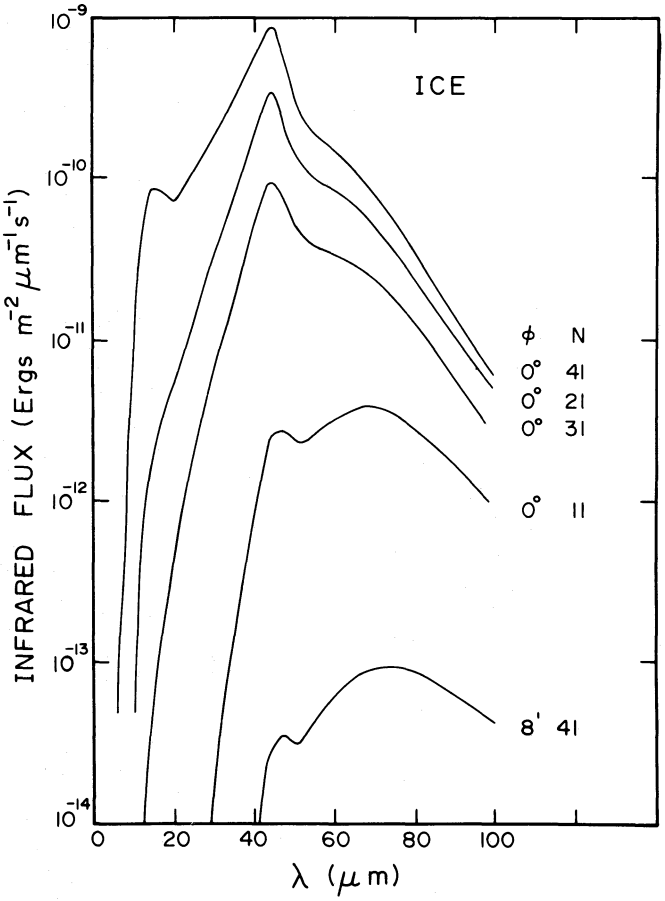

FIG. 3.—The expected infrared flux, due to thermal radiation from the ice grains within the nebula, received within the telescope aperture. Note that $a_0 = 0.5$ μm, and $n_H = 1$.

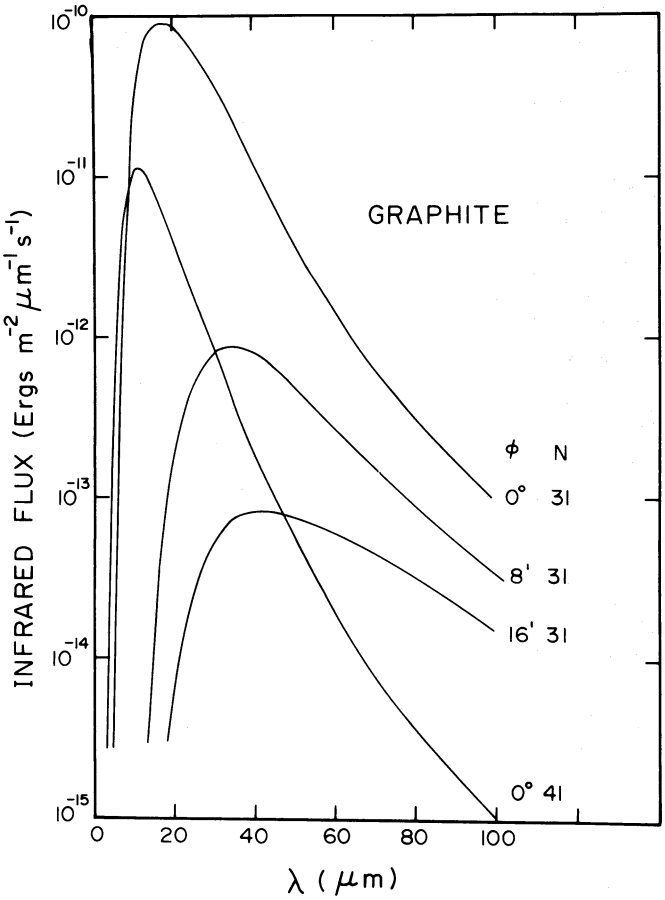

FIG. 4.—The same as in Fig. 3 but for graphite grains with $a_0 = 0.2$ μm.

comes through the assumption of a constant ratio of the grain number density to n_H. Note that the infrared fluxes for $\phi = 8'$ and $N = 11(10)41$ are almost identical. When $\phi = 0°$ and $\lambda \gtrsim 80$ μm, the fluxes are comparable for all $N = 21(10)41$.

The graphite grains give relatively far smoother curves for the nebular infrared fluxes as shown in Figure 4. Here we have $a_0 = 0.2$ μm. The maximum infrared flux for $\phi = 0$, $N = 11$, turns out to be $\sim 2.7 \times 10^{-13}\, n_H$ W m^{-2} μm^{-1} sr^{-1} at $\lambda \approx 24$ μm. Not only does the peak value go down as ϕ increases but its position also shifts toward longer wavelength for the same N. However, if $\phi = 0°$, and d_{min} decreases, the peak flux not only increases but its position also progressively shifts toward shorter wavelengths. Beyond certain wavelength, say $\lambda \gtrsim 40$ μm, the infrared fluxes are comparable for all $N = 11(10)41$ and for all ϕ's including $\phi = 0°$.

The expected infrared fluxes from the model reflection nebula containing olivine silicate grains with $a_0 = 0.5$ μm have been shown in Figure 5. Normally one considers the ice and silicate grains under the class of dielectric materials. However, the infrared spectra of the thermal radiation from olivine silicate grains in Figure 5 show some features drastically different compared to ice (dielectric) and graphite (metallic) grains. The differences arise inherently from the optical properties of these materials in the infrared. For $N = 11(10)41$, and $\phi = 0°$, there are many prominent emission and absorption features. If N is fixed at 11 and ϕ is increased to $\phi = 8'$ and $16'$, there are still several maxima and minima which nearly have a one-to-one correspondence for $\phi = 8'$ and $16'$ but not shared by the case of $\phi = 0°$. The maximum flux for $\phi = 0°$ varies from $\sim 6.4 \times 10^{-13}\, n_H$ W m^{-2} μm^{-1} sr^{-1} at $\lambda \approx 34$ μm to $\sim 3 \times 10^{-11}\, n_H$ W m^{-2} μm^{-1} sr^{-1} at $\lambda \approx 22$ μm as N goes from 11 to 41. For sufficiently large wavelengths, say $\lambda \gtrsim 60$ μm, the infrared fluxes are comparable for all $N = 11(10)41$ and perhaps independent of ϕ.

V. DISCUSSION AND CONCLUSION

Zappala (1973) has observed that the stars in the Pleiades cluster exhibit color excess in $V - [2.2\ \mu m]$ independent of interstellar reddening. It has been suggested that the comparatively young stars in Pleiades are still surrounded by circumstellar material at temperatures of ~ 500 K and moderate optical depth. Therefore, it may become necessary to examine the question of

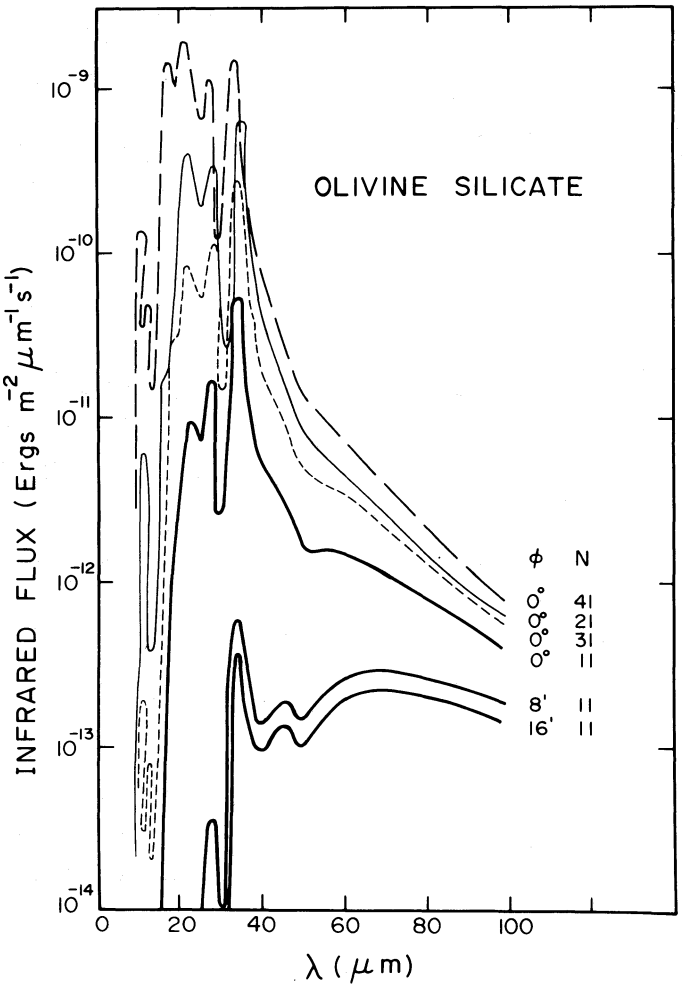

FIG. 5.—The same as in Fig. 3 except that the grains are composed of olivine silicate.

thermal emission by this kind of circumstellar grains around Merope and its role in modifying the colors and polarization in the visual and in particular the near-infrared flux from the reflection nebula.

As mentioned by Jura (1977), the measurement of the amount of far-infrared light relative to the scattered light from the nebula may tell us something about the albedo of the grains in the visual and ultraviolet. Jura has also emphasized that observations in the near-infrared, including the polarization, may be very useful for resolving the difficult question about the geometry of the nebula. In the present work we have adopted the geometry with the star within the nebula. However, the other cases of the star behind and in front of the nebula can be examined if future detailed observations so warrant. Among other reflection nebulae of interest in the far-infrared are NGC 2023, NGC 2068, NGC 7023, and R associations—for example, Canis Major R1 and Monoceros R2.

It is quite possible that the grains within the Merope reflection nebula are segregated (sieved) by size due to radiation pressure and evaporation near the illuminating hot star. Arny (1977) has considered such effects for a nebular dust cloud streaming through the Pleiades cluster. He has pointed out that the grains found near the star would differ systematically from those found in normal interstellar clouds partly because of selectively larger radiation pressure acting on larger grains and partly because of evaporation in the vicinity of the hottest star. The size differences may result in colors, polarization, and infrared fluxes across the nebula quite different from those with the case of homogeneous distribution of the grains.

The simple model of the reflection nebula presented here has revealed some interestingly distinguishable structures in the infrared fluxes emanating from the ice, graphite, and silicate grains. A plausible rough estimate for the highest flux, common for all compositions of the grains, can be given as $\sim 5(10^{-13}$ to $10^{-11})\, n_{\rm H}$ W m^{-2} μm^{-1} sr^{-1}, corresponding to the offset angle $\phi = 0°$, $n_{\rm H}$ being the hydrogen number density within the nebula. Here it is assumed that the grains continue to exist uniformly from a radial distance of ~ 0.01 pc from the star

to the boundary of the nebula. It may be noted that the factor n_H for the Merope reflection nebula can be as large as 10^3 cm^{-3} (Greenberg 1978). Thus, it is not unreasonable to expect observable infrared fluxes in the appropriate wavelength range, at least in the direction toward the star Merope. Finally, since the main contribution to the infrared flux comes from the elementary slab nearest to the star, one may be able to measure infrared linear and circular polarization as well across the nebula.

One of us (G.A.S.) would like to thank Dr. M. K. V. Bappu for continuous encouragement. We are also grateful to Professors B. J. Bok and M. K. V. Bappu for reading the manuscript and for valuable suggestions.

APPENDIX

ANALYTICAL RELATIONS OF THE GEOMETRICAL MODEL

The nebular slab represented between the plane-parallel boundaries X_1X_2 and Y_1Y_2 in Figure 1 has been divided uniformly into N elementary slabs each of thickness ΔZ. The telescope axis is represented by $OPP''P'$. The observer and the illuminating star are located at O and S, respectively. The plane through $L''P''C''$ is drawn in such a manner that the volumes corresponding to $M''N''N'M'$ and $MNN''M''$ are equal. C'', the center of the elliptical cross section with major axis $M''N''$, has been chosen as the point of symmetry for the volume element $MNN'M'$. The distance, h, between the observer and the bottom of the jth elementary slab is given by

$$h = (D - H) + (j - 1)\Delta Z\,, \qquad j = 1, 2, \ldots N\,. \tag{7}$$

Let

$$OC'' = l_1\,, \quad SC'' = l_2 = l_{2R}\,, \quad OL = h\,,$$
$$LL'' = \delta\,, \quad P''C'' = \gamma\,, \quad C_1C'' = l_{1R}\,,$$
$$\phi = \measuredangle SOP\,, \quad \phi_1 = \measuredangle POC$$
$$\alpha = \measuredangle L_NSP''\,, \quad \alpha_1 = \measuredangle P''SC''\,.$$

The small positive corrections α_1 and ϕ_1 need to be applied to α and ϕ, respectively, because the symmetry center C'' does not lie exactly on the telescope axis except when $\phi = 0°$.

The distances l_1, l_2, l_{1R}, l_{2R} for particular values of ϕ and j can be found from the following sequence of relations (Shah and Krishna Swamy 1978):

$$\delta = h\left\{\left[\frac{1 + (1 + \Delta Z/h)^3}{2}\right]^{1/3} - 1\right\}, \tag{8}$$

$$\gamma = \frac{(h + \delta)\tan\phi\tan^2\beta}{\cos^2\phi - \sin^2\phi\tan^2\beta}\,, \tag{9}$$

$$\tan(\phi + \phi_1) = \tan\phi + \gamma/(h + \delta)\,. \tag{10}$$

The two cases must be distinguished for $(h + \delta) > D$ and $(h + \delta) < D$.

Case (a): $(h + \delta) > D$

Figure 1 corresponds to this case:

$$\tan(\alpha + \alpha_1) = [\gamma + (h + \delta)\tan\phi]/(h - D + \delta)\,, \tag{11}$$

$$l_1 = (h + \delta)/\cos(\phi + \phi_1)\,, \tag{12}$$

$$l_{1R} = (h + H + \delta - D)/\cos(\phi + \phi_1)\,, \tag{13}$$

$$l_2 = l_{2R} = (h - D + \delta)/\cos(\alpha + \alpha_1)\,. \tag{14}$$

Case (b): $(h + \delta) < D$

Note that Figure 1 would be somewhat modified in this case:

$$\tan(\alpha + \alpha_1) = [\gamma + (h + \delta)\tan\phi]/(D - h - \delta)\,. \tag{15}$$

The quantities l_1 and l_{1R} have the same expressions as in case (*a*);

$$l_2 = l_{2R} = (D - h - \delta)/\cos(\alpha + \alpha_1)\,. \tag{16}$$

The exact volume of the element corresponding to $MNN'M'$ can be expressed as

$$\Delta V = h^2 \Delta Z \Delta\Omega \frac{1 + \Delta Z/h + \frac{1}{3}(\Delta Z/h)^2}{(\cos^2 \phi - \sin^2 \phi \tan^2 \beta)^{3/2}} . \quad (17)$$

If $\beta \approx 0°$ and $(\Delta Z/h) \ll 1$, this volume element approximates to the expression given by Greenberg and Roark (1967).

REFERENCES

Andriesse, C. D., Piersma, Th. R., and Witt, A. N. 1977, *Astr. Ap.*, **54**, 841.
Arny, T. 1977, *Ap. J.*, **217**, 83.
Elvius, A., and Hall, J. S. 1966, *Lowell Obs. Bull.*, **6**, 257.
———. 1967, *Lowell Obs. Bull.*, **7**, 17.
Emerson, J. P., Furniss, I., and Jennings, R. E. 1975, *M.N.R.A.S.*, **172**, 411.
Field, G. B., Partridge, R. B., and Sobel, H. 1967, in *Interstellar Grains*, ed. J. M. Greenberg and T. P. Roark (NASA SP-140), p. 207.
Greenberg, J. M. 1978, in *Cosmic Dust*, ed. J. A. M. McDonnell (New York: Wiley), p. 187.
Greenberg, J. M., and Roark, T. P. 1967, *Ap. J.*, **147**, 917.
Huffman, D. R. 1975, *Ap. Space Sci.*, **34**, 175.
Huffman, D. R., and Stapp, J. L. 1973, in *IAU Symposium 52, Interstellar Dust and Related Topics*, ed. J. M. Greenberg and H. C. van de Hulst (Dordrecht: Reidel), p. 297.
Irvine, W. M., and Pollack, J. B. 1968, *Icarus*, **8**, 324.
Jura, M. 1977, *Ap. J.*, **218**, 749.
———. 1979, *Ap. J.*, **231**, 732.
Kolesnik, I. G. 1978, *Soviet Astr.*, **22**, 566.
Krishna Swamy, K. S. 1970, *Astr. Ap.*, **8**, 358.
Low, F. J. 1977, in *Infrared and Submillimeter Astronomy*, ed. G. G. Fazio (Dordrecht: Reidel), p. 3.
Markkanen, T. 1977, *Astr. Ap.*, **56**, 83.
Savage, B. D., and Mathis, J. S. 1979, *Ann. Rev. Astr. Ap.*, **17**, 73.
Shah, G. A. 1974, *Pramana*, **3**, 338.
———. 1977*a*, *Astr. Nachr.*, **298**, 319.
———. 1977*b*, *Pramana*, **9**, 461.
———. 1977*c*, *Kodaikanal Obs. Bull., Ser. A*, **2**, 42.
Shah, G. A., and Krishna Swamy, K. S. 1978, *Kodaikanal Obs. Bull., Ser. A*, **2**, 95.
———. 1979, *Kodaikanal Obs. Bull., Ser. A*, **2**, 195.
Taft, E. A., and Philipp, H. R. 1965, *Phys. Rev.*, **138A**, 197.
van de Hulst, H. C. 1957, *Light Scattering by Small Particles* (New York: Wiley).
Voshchinnikov, N. V. 1977, *Soviet Astr.*, **21**, 693.
———. 1978, *Soviet Astr.*, **22**, 561.
Watson, W. D. 1975, in *Atomic and Molecular Physics and Interstellar Matter*, ed. R. Balian, P. Encreanas, and J. Lequeux (Amsterdam: North-Holland).
Zappala, R. R. 1973, *Ann. Rept. Hale Observatories*, 1972–1973, p. 110.

G. A. SHAH: Indian Institute of Astrophysics, Koramangala, Bangalore—560 034, India

K. S. KRISHNA SWAMY: Tata Institute of Fundamental Research, Homi Bhabha Road, Bombay—400 005, India